Vulnerability Assessment of Deteriorated Bridges Under Seismic Events

B. Shafei
Assistant Professor
Department of Civil and Environmental Engineering
University of Massachusetts Amherst, USA

A. Alipour
Assistant Professor
Department of Civil and Environmental Engineering
University of Massachusetts Amherst, USA

SUMMARY:
Reinforced concrete (RC) bridges are usually subjected to various natural hazards and environmental stressors during their life-cycle. There are several studies currently available in the literature on the performance of RC bridges solely under a specific natural hazard, such as an earthquake or wind, or a particular environmental stressor, such as corrosion or carbonation. But in of all real conditions, the simultaneous effects of these phenomena must be recognized to obtain a more accurate assessment of bridge vulnerability. Towards this goal, the current paper proposes a vulnerability assessment process through a multi-hazard framework. This process provides engineers and decision-makers with a probabilistic estimation of the bridge damageability under seismic events while the bridge is continuously exposed to the corrosive environment. This framework is extendable to the other combinations of hazards and stressors and can help to improve the risk and reliability analysis of various bridge systems.

Keywords: seismic analysis, structural performance assessment, deterioration, reinforced concrete bridge

1. INTRODUCTION

Chloride-induced corrosion in reinforced concrete (RC) bridges is a mechanism caused by the intrusion of chloride ions into concrete. This mode of corrosion is more probable when RC bridges are located in coastal regions and exposed to aggressive environmental conditions. Because of the penetration of chloride ions in structural members, the chloride content of concrete gradually increases and when the concentration of chloride ions in the pore solution on the vicinity of reinforcing bar reaches a threshold value, the chloride-induced corrosion initiates. Chloride transport mechanism in concrete is a complex phenomenon that may occur in several forms, such as ionic diffusion, capillary suction, and permeation. The rate of this mechanism depends on the characteristics of concrete, degree of pore saturation, chloride binding capacity, free chloride content, and exposure conditions. By increasing the duration of time through which a bridge is exposed to aggressive conditions, the deterioration process of reinforcing bars can get relatively fast. This results in cracking or spalling of RC members and may lead to severe reduction in serviceability of bridges.

The time between corrosion initiation and serviceability failure is usually smaller than the required time for corrosion to initiate. Therefore, the realistic estimation of corrosion initiation time has a significant role in the accurate performance prediction of RC bridges over the time. In the present paper, an integrated computational framework is proposed to simulate the penetration of chloride ions into concrete. Towards this goal, the effects of various parameters, such as water to cement ratio, ambient temperature, relative humidity, age of concrete, free chloride content, and chloride binding capacity, are considered to calculate the chloride content in different time intervals. It can be seen that by increasing the time during which a bridge is exposed to the aggressive conditions, the deterioration process of reinforcing bars can become relatively fast. This results in the cracking and spalling of the concrete in addition to reduction in the mass and effective cross section of the reinforcing bars. The

structural performance of a set of short-, medium-, and long-span bridges are evaluated using probabilistic lifetime fragility analysis over a life cycle of 30 years and the effects of variation in corrosion initiation time on the fragility parameters are studied.

2. CHLORIDE INTRUSION

To study the chloride intrusion process, different empirical and numerical models have been proposed during the past three decades. The majority of these models are based on the solution of Fick's second law (Tuutti 1982) as expressed in Eqn. 1.

$$C_{Cl}(x,t) = C_S\left[1 - \mathrm{erf}\left(\frac{x}{2\sqrt{D_{Cl}t}}\right)\right] \quad (1)$$

where $C_{Cl}(x,t)$ = total chloride content at the spatial coordinate x and time t; C_s = surface chloride content; D_{Cl} = diffusion coefficient; and *erf* (.) = error function. In order to obtain a closed-form analytical solution for the total chloride content (Eqn. 1), it is assumed that the diffusion coefficient as well as boundary conditions is constant over the time. Chatterji (1995) and Kong et al. (2002) have questioned the accuracy of this equation for two main reasons: first, the chloride diffusion coefficient and boundary conditions are assumed to be constant while they may vary over the time; and second, the solution is formulated in terms of total chloride concentration while in reality only free chloride ions are responsible for corrosion initiation in concrete.

In order to improve the Eqn. 1, Saetta et al. (1993) developed a numerical approach using the conventional diffusion theory (Fick's first law) and the mass conservation principle to model the chloride diffusion into concrete. In the proposed diffusion process, the coupling between moisture and heat flow is based on a model proposed by Bažant and Najjar (1972). Xi and Bažant (1999) also suggested a model for chloride penetration in saturated concrete, which was dominated by binding capacity and chloride diffusivity. Later on, Kong et al. (2002) used the Xi and Bažant's model to examine the rate of chloride ingress into concrete by taking into account the influence of water to cement ratio and curing time. Ababneh et al. (2003) extended the work of Xi and Bažant by developing a mathematical model for chloride penetration in non-saturated concrete by considering the binding capacity, chloride diffusivity, and moisture diffusivity. In this paper, the authors have extended the numerical model so that it considers the effects of chloride binding capacity, free chloride content, ambient temperature, and relative humidity in addition to concrete aging.

2.1. Modeling of Chloride Diffusion Process

It is assumed that the dominant mode of chloride intrusion into concrete is diffusion. The diffusion is the motion of chloride ions within the pore solution in response to the ion concentration gradient, which is described with the Fick's first law based on the mass conservation principle. The chloride ions concentrated on the exposed concrete surface diffuse into cement matrix due to the ion concentration gradient and this diffusion into partially saturated concrete can be described using the following partial differential equation (Saetta et al. 1993):

$$\frac{\partial C_f}{\partial t} = -\mathrm{div}\left[\frac{D_{Cl}}{1 + (1/w_e)(\partial C_b / \partial C_f)}\nabla(C_f)\right] \quad (2)$$

where C_f = free chloride concentration in the unitary volume of porous body (kg/m^3 of concrete); t = time; w_e = evaporable water content; and ($\partial C_b/\partial C_f$) = chloride binding capacity in which C_b is the bound chloride content. The chloride binding capacity characterizes the relationship between free and bound chloride ions in concrete at a specific temperature and it is also referred to as the "binding

isotherm". Martin-Perez et al. (2001) studied three different binding isotherms for concrete, including: idealized linear, Langmuir, and Freundlich binding isotherms. The proposed relationships for these isotherms along with the suggested coefficient values for RC bridges located in coastal areas can be found in Table 1.

Table 1. Three different binding isotherms

Isotherm	C_b	$\partial C_b/\partial C_f$	α	β
Linear	αC_f	α	0.07	-
Langmuir	$\alpha C_f/(1+\beta C_f)$	$\alpha/(1+\beta C_f)^2$	0.39	0.07
Freundlich	αC_f^{β}	$\alpha\beta C_f^{\beta-1}$	1.05	0.36

Given the relationship between free and bound chloride content, the total chloride content, C_t, of the concrete can be expressed as the summation of these values.

$$C_t = C_b + w_e C_f \tag{3}$$

2.2. Chloride Diffusion Coefficient

The diffusion coefficient in Eqn. 2 is calculated by taking into account the contribution of all influential parameters, as below:

$$D_{Cl} = D_{Cl,ref}\, F_2(T)\, F_3(h)\, F_4(t_e)\, F_5(C_f) \tag{4}$$

where $D_{Cl,ref}$ = chloride diffusion coefficient estimated at a reference temperature and humidity. In Eqn. 4, $F_2(T)$ accounts for the dependence of chloride diffusion coefficient on temperature T; $F_3(h)$ represents the influence of relative humidity h; $F_4(t_e)$ denotes the effect of concrete age t_e; and $F_5(C_f)$ considers the influence of free chloride content on the diffusion process. To evaluate the extent of contribution of mentioned parameters in Eqn. 4, the following mathematical expressions are suggested (Bamforth and Price 1996, Saetta et al. 1993, Xi and Bažant 1999, Bažant and Najjar 1972, Martin-Perez et al. 2001, and Kong et al. 2002):

(1) Reference chloride diffusion coefficient:

$$\log D_{Cl,ref} = a + b \log(w/c) \tag{5}$$

where a and b = empirical factors, here assumed equal to -10.6 and 1.9; and w/c = water to cement ratio, assumed equal to 0.5 in this paper.

(2) Temperature effects:

$$F_2(T) = \exp\left[\frac{E}{R}\left(\frac{1}{T_{ref}} - \frac{1}{T}\right)\right] \tag{6}$$

where E = activation energy, equals to 44.6 ± 4.3 (kJ/mol) for w/c = 0.5; R = gas constant, equals to 8.314 (kJ/mol.˚ K); T_{ref} = temperature at which reference chloride diffusion coefficient, $D_{cl,ref}$, is measured, equals to 296˚K; and T = absolute ambient temperature at the location of bridge, obtained from available data.

(3) Humidity effects:

$$F_3(h) = 1 \Big/ \left[1 + \left(\frac{1-h}{1-h_c} \right)^4 \right] \tag{7}$$

where h_c = humidity level at which D_{Cl} drops halfway between its maximum and minimum values, equals to 0.75; and h = relative humidity at the location of bridge, obtained from available data.

(4) Effects of concrete age:

$$F_4(t_e) = \left(\frac{t_{ref}}{t} \right)^m \tag{8}$$

where t_{ref} = reference time, equals to 28 day; m = empirical age factor, equals to 0.04; and t = actual time of exposure.

(5) Effects of free chloride content:

$$F_5(C_f) = 1 - \kappa (C_f)^n \tag{9}$$

where empirical parameters, κ and n, are assumed equal to 8.33 and 0.5, respectively.

Considering the influential parameters mentioned above, the time-varying diffusion coefficient at the reinforcing bar level is calculated using Freundlich isotherm (Fig. 1). The strong fluctuation of chloride diffusion coefficient is resulted from $F_2(T)$ and $F_3(h)$, due to the seasonal variations in the ambient temperature and relative humidity, respectively.

Because of dependence of D_{Cl} on nonlinear, time-dependent parameters (Eqn. 4), the governing partial differential equation given by Eqn. 2 cannot be solved without using numerical methods. The current study develops a finite difference algorithm to solve the partial differential equation of chloride diffusion process as a boundary value problem. This helps to study the effects of all influential parameters at different time intervals and results in more accurate estimation of corrosion initiation time. Using the finite difference algorithm, a set of equations is solved simultaneously in each time step until a specified chloride threshold value is reached. The time corresponding to this threshold indicates the corrosion initiation time.

The initial conditions and boundary values used for the numerical solution are expressed as below:

$$\begin{cases} t = 0: \quad C_f = 0 \quad at \;\; x > 0 \\ t \geq 0: \quad C_f = C_S \;\; at \;\; x = 0 \end{cases} \tag{10}$$

where C_s = surface chloride content. The surface chloride content may depend on the composition of concrete, the location of structure, the orientation of its surface, the chloride concentration in the environment, and the general conditions of exposure with regard to rain and wind (Bertolini 2008). To determine the range of surface chloride content, McGee (1999) conducted a field-based study of 1158 bridges in Australian state of Tasmania. He suggested that the surface chloride content is a function of distance from the coast, d, and for the structures located on the coast lines ($d < 0.1$ km), the C_s value is 2.95 kg/m^3. Val (2004) also collected some surface chloride content data from Mediterranean coasts and proposed a value of 7 kg/m^3. In this paper, an average value of 5 kg/m^3 is assumed for C_s.

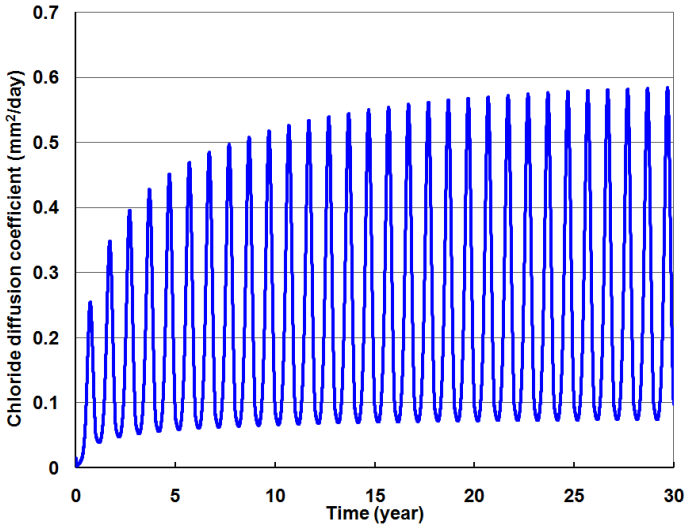

Figure 1. Chloride diffusion coefficient, calculated using Freundlich isotherm

2.3. Corrosion Initiation Time

The time to corrosion initiation is determined as the time when the chloride concentration near reinforcing bars (at a depth equals to the concrete cover depth) reaches the threshold chloride concentration, $C_{critical}$. The threshold total chloride content for this study is taken as the 1 % of cement weight, assumed equal to 350 kg/m^3. The values of free, bound, and total chloride content through a 30-year period of exposure at the cover depth level of 50 mm is depicted in Fig. 2 for Freundlich isotherm.

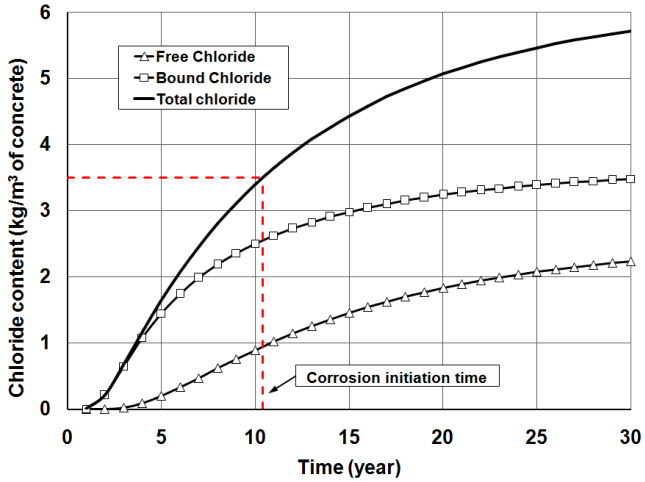

Figure 2. Free, bound, and total chloride content at the rebar level, calculated using Freundlich isotherm

Considering the total chloride content profile in Fig. 2, the corrosion initiation time is estimated by finding the intersection of chloride profile and the threshold value (3.5 kg/m^3). In the current case, it can be seen that the corrosion initiation time is equal to 10.40 years. By repeating the same procedure using the other two isotherms, i.e. linear and Langmuir isotherms, the corrosion initiation time would change to 9.33 and 12.66 years, respectively. These values of corrosion initiation time are within the usually observed range of 7 to 20 years, as suggested by Kong et al. (2002).

3. STRUCTURAL DEGRADATION DUE TO CORROSION

After the corrosion initiation time, the protection film of the reinforcing bar is depassivated and the transport of iron ions starts. This results in the formation of rust layers around the rebar during the corrosion process. This process continues until the volume of rust reaches a level that causes the concrete to crack due to the excessive expansion of rust layers. In this study the crack initiation time is calculated using the Faraday's law which relates the mass of steel consumed over the time to the amount of current that flows through the electrochemical corrosion cell. The rate of mass loss per unit length of bar subjected to the corrosion, ΔM_{loss} (gr/cm), for a time step of Δt (sec) can be described as:

$$\Delta M_{loss}(t) = k\pi D(t) i_{corr} \tag{11}$$

where $D(t)$ = reduced diameter of reinforcing bar during the corrosion process; k = mass transport coefficient equal to 2.893×10^{-9}; and i_{corr} = current per unit area of the reinforcing bar. For the i_{corr} in Eqn. 11, a range of 10 to 25 $\mu A/cm^2$ has been suggested by Rodriguez et al. (1994). This range corresponds to the high reinforcement corrosion risk because it is larger than 1 $\mu A/cm^2$ (Andrade et al., 1993). In the current study, i_{corr} is assumed to be equal to 10 $\mu A/cm^2$. By taking the steel mass density, ρ_s, equal to 7.8 (gr/cm^3), the change in the volume of corroded steel, ΔV_{loss} (cm^3/cm), can be simply calculated from ΔM_{loss}. The reduced rebar diameter after each time step of corrosion is calculated as:

$$D(t) = \sqrt{D_0^2 - \Delta V_{loss}(t)} \tag{12}$$

where D_0 is the initial diameter of the rebar.

The residual strength of corroded reinforcing bars was investigated experimentally by Du et al. (2005a and b). They conducted both accelerated and simulated corrosion tests on the bars embedded in the concrete and concluded that the strength of steel bars decreases significantly with chloride penetration. Their test results are in reasonable agreement with other studies, such as Andrade et al. (1993), Lee et al. (1996), and Morinaga (1996). Therefore, the below empirical equation proposed by Du et al. (2005a and b) is used to estimate the time-dependent loss of yield strength in corroded reinforcing bars:

$$f_y(t) = (1 - 0.005m(t)) \tag{13}$$

where $f_y(t)$ is the yield strength of corroded reinforcement at each time step, f_{y0}, the yield strength of non-corroded reinforcement, t, the time elapsed since corrosion initiation (year), and $m(t)$, the percentage of steel mass loss over the time. The $m(t)$ is equal to the consumed mass of steel per unit length divided by the original steel mass. The reduced diameter and the remaining yield strength of rebars are calculated at different time steps during the life-cycle of the bridge (Table 2). These values are used to update the characteristics of bridge models during the structural capacity estimation and seismic performance evaluation of corroded bridges.

Table 2. Reduction in the mass, diameter, and yield strength of reinforcing bars at 5-year time intervals

Time* (year)	**0**	**5**	**10**	**15**	**20**	**25**	**30**	**35**	**40**	**45**	**50**
M_{loss}/M_0 (%)	0.00	6.38	12.24	18.10	23.96	29.82	35.68	41.54	47.40	53.26	59.12
D (mm)	35.80	34.75	33.61	32.46	31.32	30.17	29.03	27.88	26.74	25.59	24.45
f_y/f_{y0}	1.00	0.97	0.94	0.91	0.88	0.85	0.82	0.79	0.76	0.73	0.70

*after corrosion initiation

Through a step-by-step analysis, the time in which the concrete starts cracking is determined as the time when the percentage of steel mass loss, $m(t)$, becomes equal to a critical level, m_{critical}. The m_{critical} which can be defined as a function of rebar dimensions and concrete properties (El Maadawy and Soudki, 2007) is calculated in the present study equal to 20%. Based on this critical level, the crack initiation time is found to be 51 days (0.14 year) for the structures under consideration. To calculate the crack width after crack initiation, w_{crack} (mm), the analytical equation proposed by Vidal et al. (2004) can be used:

$$w_{crack}(t) = K_{crack}(\Delta A_s(t) - \Delta A) \tag{14}$$

where $\Delta A_s(t)$ is the steel loss of the rebar cross section during the corrosion process (mm^2), ΔA_0, the steel loss of the cross section needed for crack initiation (mm^2), and K_{crack}, an empirical coefficient equal to 0.0577. Assuming the crack width of 0.3 mm as one of the first serviceability limits, the time in which this limit is exceeded has been calculated to equal 117 days (0.32 year). Comparing the time to crack initiation (0.14 year) and the time to exceed the crack width of 0.3 mm (0.32 years) with the time to corrosion initiation (10.40 years), it can be clearly seen that the two former times are negligible within the whole life-cycle of the bridge. Hence, considering the fact that the crack initiation occurs shortly after the corrosion initiation time, this paper assumes that the time corresponding to the serviceability threshold is equal to the corrosion initiation time. Furthermore, it is widely accepted that a crack width of more than 1 mm indicates the performance failure of the concrete cover. The time required for reaching this crack width limit has also been calculated to equal 542 days (1.48 year) after corrosion initiation. Since the capacity of structures under study will be evaluated every 5 years after the corrosion initiation time, it is assumed that the concrete cover is destroyed from the first analysis interval.

4. SEISMIC PERFORMANCE ASSESSMENT

To examine the effects of probabilistic estimation of corrosion initiation time on the capacity prediction of bridges, a set of typical bridges located in coastal areas are modeled and analyzed to determine the remained structural capacity at the end of 30-year life cycle of bridge. These bridges include three two-span bridges with 15, 30, and 45 m span lengths representing short-, medium-, and long-span bridges, respectively. All the bridge cases are assumed to have two-column bents and fixed foundations. The column height is equal to 10 m and the deck cross-sectional area is 12 m^2. The schematic view of these bridges is shown in Fig. 3. The bridges under consideration are numerically modeled using OpenSees (2009). The bridge models consist of a detailed model of columns with fiber-discretized cross sections, elastic deck sections, and simplified abutment springs.

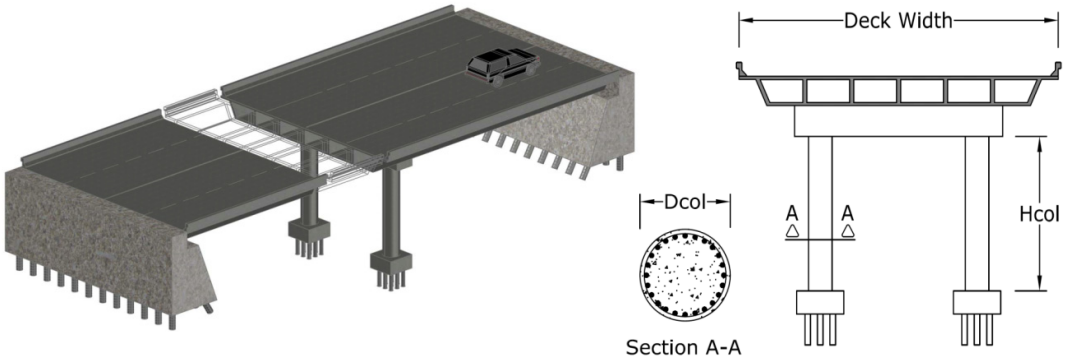

Figure 3. A schematic view of the two-span case-study bridges

The structural degradation occurs only after the corrosion initiation time. When corrosion initiates, the protective film on the reinforcing bar is depassivated and the rebar cross section decreases due to the consumption of steel in corrosion process. A short time is usually required for corrosion products to expand such that the concrete cover starts cracking. Considering the decrease in rebar cross-section, concrete cover, and steel yield strength due to the deterioration process, a significant structural capacity loss is expected for bridges after the onset of corrosion.

To perform fragility analysis, the column curvature ductility is taken here as the primary damage measure. The curvature ductility is defined as the ratio of maximum column curvature recorded from a nonlinear time-history analysis to the column yield curvature obtained from moment-curvature analysis. Following the procedure given by Priestley et al. (1996), the curvature ductility values of all the bridge cases are calculated under the set of 60 ground motions and then compared with damage limit states. In this study, the damage limit states are assumed to equal the ductility of 1.0, 2.0, 4.0, and 7.0 for the slight, moderate, extensive, and complete damage states, respectively. The estimation of these limit states are beyond the scope of this paper, but the suggested values are in accordance with the limit states available in the literature for similar bridges (Hwang et al. 2000 and Yang et al. 2009).

Under a ground motion excitation with the peak ground acceleration of PGA_i (here i = 1, ..., 60), the parameters of each fragility curve (i.e., median, c_k and log-standard deviation, ζ_k) are estimated using the maximum likelihood procedure given in Shinozuka et al. (2000):

$$F_k(PGA_i \mid \zeta_k, c_k) = \Phi[\frac{\ln(PGA_i / c_k)}{\zeta_k}] \tag{15}$$

where F_k is the probability of exceeding the damage state of k and $\Phi[.]$ is the standard normal distribution function. To evaluate the effects of chloride-induced corrosion on the seismic damageability of RC bridges, the fragility curves are generated for the case-study bridges at different time steps during their life-cycle. Considering the extent of structural degradation, the median and log-standard deviation of fragility curves is estimated for the corroded bridges. The time-dependent fragility curves of the two-span bridges with the medium span length and column height of 10.0 m are depicted in Fig. 4. It can be understood from this figure that for a specific PGA value, the probability of exceeding any damage state increases over the time due to the corrosion process. This increases the seismic damageability of bridge and makes it more vulnerable to natural hazards.

5. CONCLUSIONS

This paper provides a computational framework to improve the life-cycle design and performance assessment of reinforced concrete bridges subjected to multiple natural hazards and environmental stressors. While bridges under consideration are located in seismic areas, they are continuously exposed to the attack of chloride ions. The complexity of this situation makes it necessary to simultaneously study a natural hazard and an environmental stressor over the time. Towards this goal, the current research first establishes a detailed computational approach that examines the chloride-induced corrosion by taking into account all the major influential parameters. The extent of structural degradation due to the corrosion process is calculated to update the properties of structural members during the life-cycle of the bridge. Based on the characteristics of corroded bridges, seismic performance of a group of case-study bridges with different structural attributes is evaluated and the level of performance reduction is quantified using age-dependent seismic fragility curves.

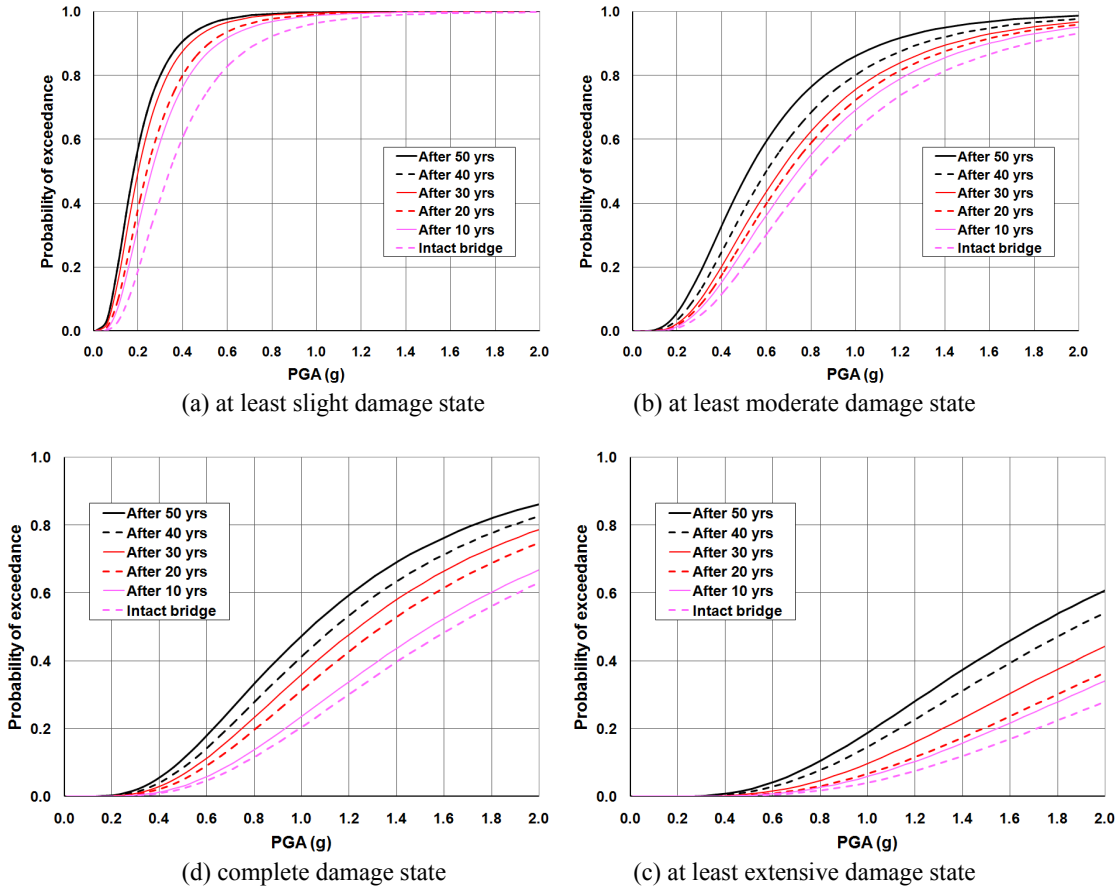

Figure 4. Time-dependent fragility curves for the two-span bridge with the medium span length and column height of 10 m

REFERENCES

Ababneh, A., Benboudjema, F., and Xi, Y. (2003). Chloride penetration in non-saturated concrete, *Journal of Materials in Civil Engineering*, **15: 2**, 183-191.

Andrade, C., Alonso, C., and Molina, F.J. (1993). Cover cracking as a function of rebar corrosion: Part I: Experimental test, *Materials and Structures*, **26: 3**, 345-353.

Bamforth, P.B., and Price, W.F. (1996). An international review of chloride ingress into structural concrete, Report No. 1303/96/9092, Taywood Engineering Ltd. technology division, Middlesex, U. K.

Bazant, Z.P., and Najjar, L.J. (1972). Nonlinear water diffusion in unsaturated concrete, *Materials and Structures*, **5: 25**, 3-20.

Bertolini, L. (2008). Steel corrosion and service life of reinforced concrete structures, *Structure and Infrastructure Engineering*, **4: 2**, 123-137.

Chatterji, S. (1995). On the probability of Fick's second law to chloride ion immigration through Portland cement concrete, *Cement and Concrete Research*, **25: 2**, 299-303.

Du, Y.G., Clark, L.A., and Chan, A.H.C. (2005a). Residual capacity of corroded reinforcing bars, *Magazine of Concrete Research*, **57: 3**, 135-147.

Du, Y.G., Clark, L.A., and Chan, A.H.C. (2005b). Effect of corrosion on ductility of reinforcing bars, *Magazine of Concrete Research*, **57: 7**, 407-419.

El Maaddawy, T., and Soudki, K. (2007). A model for prediction of time from corrosion initiation to corrosion cracking, Cement and Concrete Composites, **29: 3**, 168-175.

Hwang, H., Liu, J.B., and Chiu, Y-H. (2001). Seismic fragility analysis of highway bridges, Center of Earthquake Research and Information, University of Memphis, Tennessee, USA.

Kong, J.S., Ababneh, A.N., Frangopol, D.M., and Xi, Y. (2002). Reliability analysis of chloride penetration in saturated concrete, *Journal of Probabilistic Engineering Mechanics*, **17: 3**, 302-315.

Lee, H.S., Tomosawa, F., and Noguchi, T. (1996). Effect of rebar corrosion on the structural performance of single reinforced beams, Durability of Building Material and Components, E & FN Spon, London, U.K.
Mc Gee, R. (1999). Modeling of durability performance of Tasmanian bridges, Proceedings of the ICASP8 Conference, Sydney, Australia, 297-306.
Martin-Perez, B., Pantzopoulou, S.J., and Thomas, M.D.A. (2001). Numerical solution of mass transport equations in concrete structures, *Computers and Structures*, **79: 13**, 1251-1264.
Morinaga, S. (1996). Remaining life of reinforced concrete structures after corrosion cracking, Durability of Building Material and Components, E & FN Spon, London, U.K.
OpenSees Development Team. (2009) OpenSees: Open System for Earthquake Engineering Simulation.
Priestly, M.J.N., Seible, F., and Calvi, G.M. (1996). Seismic Design and Retrofit of Bridges, John Wiley and Sons Inc., USA.
Rodriguez, J., and Ortega, L.M. (1994). Assessment of structural elements with corroded reinforcement, Corrosion and Corrosion Protection in Concrete, Sheffield Academic Press, Sheffield, U.K.
Saetta, A.V., Schrefler, B.A., and Vitaliani, R.V. (1993). The carbonation of the concrete and the mechanism of moisture, heat and carbon dioxide flow through porous materials, *Cement and Concrete Research*, **23: 4**, 761-772.
Tuutti, K. (1982). Corrosion of steel in concrete, Swedish Cement and Concrete Research Institute, Stockholm, Sweden.
Xi, Y., and Bazant, Z.P. (1999). Modeling chloride penetration in saturated concrete, Journal of Materials in Civil Engineering, **11: 1**, 58-65.